

Implementation of a smeared crack model in the finite element method and its application to two-dimensional nonlinear analysis of concrete beams

Implementación de un modelo de fisura cohesiva en el método de los elementos finitos y su aplicación al análisis no lineal bidimensional de vigas de concreto

Juan Carlos Tamásco Sandoval*; Martín Estrada Mejía* <https://orcid.org/0000-0002-3089-8857>; Dorian Luis Linero Segrera**¹ <http://orcid.org/0000-0001-8198-8839>

* University of the Andes, Bogotá - COLOMBIA

** National University of Colombia, Bogotá – COLOMBIA

Fecha de Recepción: 11/07/2023

Fecha de Aceptación: 21/03/2024

Fecha de Publicación: 30/04/2024

PAG: 63-76

Abstract

This paper describes the implementation of a two-dimensional rotating smeared crack model within the framework of a nonlinear finite element analysis code, and its application to the mechanical behavior of the plain concrete. In this work, the formulation of three concrete softening law subjected to fracture Mode-I is adapted, considering infinitesimal strains, static loads and two-dimensional conditions. The rotating smeared crack model and the three softening laws are all implemented in Fortran language, into the open source software for nonlinear finite element analysis HYPLAS. The pre- and post-process for a graphical representation of the mesh and the results are done with GMSH or GiD. Finally, three experimental tests of concrete beams of other authors are simulated. The concentration of the displacement contour lines obtained in the simulation represents the crack patterns in the solid. The relationship between the applied load and the representative displacement in each analysis step describes the mechanical response of the beam. Other computed parameters were the crack opening and the principal stresses in the solid. The numerical results were satisfactory in comparison with the experimental tests.

Keywords: Analysis of concrete structures; fracture computational mechanics; smeared crack model; finite element methods; concrete beam subjected to bending.

Resumen

Este artículo describe la implementación de un modelo bidimensional de fisura distribuida rotante en el marco del análisis no-lineal mediante el método de los elementos finitos, y su aplicación al comportamiento mecánico del concreto simple. En este trabajo se adapta la formulación general del modelo de fisura distribuida rotante para tres leyes de ablandamiento del concreto en modo I de fractura, considerando deformaciones infinitesimales, cargas estáticas y estado plano de esfuerzos o de deformaciones. Asimismo, se implementa un modelo constitutivo de fisuración distribuida y tres leyes de ablandamiento en lenguaje Fortran, dentro del programa a código abierto de análisis no-lineal por elementos finitos HYPLAS. El preproceso de mallado del dominio y el postproceso de presentación gráfica de los resultados se realiza con los programas GMSH o GiD. Finalmente, se simulan tres ensayos experimentales de vigas de concreto realizados por otros autores. La concentración de líneas de contorno del desplazamiento obtenidas en la simulación representan el patrón de fisuración en el sólido. Por otro lado, la relación entre la carga aplicada y el desplazamiento representativo en cada paso de análisis describe la respuesta mecánica de la viga. Otras entidades calculadas fueron la apertura de fisura y los esfuerzos principales en el sólido. Los resultados numéricos fueron satisfactorios en comparación con los ensayos experimentales.

Palabras clave: Análisis de estructuras de concreto; mecánica computacional de la fractura; modelo de fisuración distribuida; método de los elementos finitos; vigas de concreto sometidas a flexión.

¹ Corresponding author:

National University of Colombia, Bogotá – COLOMBIA

Corresponding author: dllineros@unal.edu.co

1. Introduction

The fracture process of the concrete can be represented with the smeared crack model, initially defined by (Rashid, 1968), who established that the inelastic strain at the fracture zone is distributed in a band around the main crack (Bazant and Planas, 1998). In this model, the crack orientation is fixed in the major principal direction when the major principal stress achieves the tensile strength. Later, this stress decreases according to the normal opening between the crack faces, representing a Mode-I fracture. In this approach, the crack can maintain inside the finite element without changing the mesh topology.

Different authors have formulated the smeared crack model, enhancing some aspects. (Suidan and Schnobrich, 1973) include the transfer of shear stress on parallel planes of the crack, preserving the direction got in the first inelastic loading step. Instead, other researchers propose the rotating smeared crack model, in which the crack direction is updated in each loading step (Rots and Blaauwendraad, 1989). In the model developed by de Borst and Nauta (de Borst and Nauta, 1985), a different non-orthogonal plane represents the crack. Subsequently, other authors use the bandwidth concept in order to scale the cracking zone size at each material point and to provide the same fracture energy (Bazant and Planas, 1998); (Jirasek and Patzak, 2001).

The rotating smeared crack model has been implemented on the finite element method, overcoming different numerical problems, until it achieves satisfactory results. For example, some works (Jirasek and Bauer, 2012); (Oliver, 1989) reduce the dependence of the material fracture energy on the finite element size and avoid the spurious stress that occurs when the orientation of the finite element sides does not match the crack direction.

The current formulation of the smeared crack model and its numerical implementation allow representing approximately the cracking process of the concrete in Mode-I fracture. Other models more complex like the strong discontinuity approach with embedded crack (Oliver, 1996) and the extended finite method with discrete crack (Zi and Belytschko, 2003), have reached greater accuracy (de Borst et al., 2004).

Some software represent the cracking process of the plain and reinforced concrete using the constitutive relationship of the smeared crack model like ATENA (Cervenka, 1985) and Vector2 (Vecchio and Collins, 1986). Likewise, several multi-physics commercial software, such as ABAQUS, ANSYS or MIDAS include modulus with this constitutive model or with continuous or discrete models of damage or plasticity that also represent the concrete behavior (Graffe and Linero, 2010); (Sakbana and Mashreib, 2020). These programs are robust and easy to use; nevertheless, the internal procedures are hidden from the user.

Open source programs of nonlinear analysis of finite elements allow implementing new routines with other constitutive models. For example, the software oofem (Jirasek and Patzak, 2001) written in C++, or the programs FEAP (Zienkiewicz et al., 2013) or HYPLAS (de Souza et al., 2008) written in Fortran.

The main objective of this work is to represent the fracture process of concrete beams in plane stress conditions, building and using an open-source program based on the rotating smeared crack model and the finite element method. This allows us to understand and modify the procedures of the numerical analysis.

The contribution of this work is the development of computational functions of a constitutive model that describes the concrete cracking, which can be simply included on a finite element code with nonlinear analysis strategy.

2. Methodology

The rotating smeared crack model is implemented as a new constitutive material model into the two-dimensional nonlinear solids analysis software HYPLAS (de Souza et al., 2008); (Tamasco, 2019). Likewise, the routines to read the finite element mesh from the pre-process module of GMSH or GiD and to write the results in the appropriate format for the post-process module on the same graphical tools were coded (CIMNE, 2000); (Geuzaine and Remacle, 2009). This nonlinear finite element analysis considers infinitesimal strain, quasi-static load, plane stress state and nonlinear material behaviour. The numerical solution is obtained through an implicit approach based on the incremental scheme of modified Newton-Raphson (de Souza et al., 2008). This scheme allows to calculate the internal forces and the tangent stiffness of each finite element during each iteration.

The steps of this research strategy consist in (i) formulating the smeared crack model to represent the fracture process of the concrete in Mode-I, (ii) formulating the constitutive model of a material point through the relationships between the stress and strain tensor, and between the constitutive tangent tensor and the strain tensor, (iii) coding and including of the previous model into nonlinear analysis scheme by finite element, using linear triangular elements, and (iv) simulating experimental test of other authors with the model and comparing its results.

2.1. Formulation of the smeared crack model

In the normal direction to the crack n , the smeared crack model establishes that: (i) the total strain ϵ_m is defined by the additive decomposition of the elastic strain ϵ_m^e and the cracking strain ϵ_m^c , (ii) the normal stress of the elastic behaviour σ_m^e and of the cracking model σ_m^c are the same σ_m , (iii) a constitutive function $F(\epsilon_m^c)$ defines the one-dimensional relationship between the cracking strain $\epsilon_{nn}^c = \epsilon_{nn} - \epsilon_{nn}^{EL}$ and the normal stress σ_m^c , where the strain in the elastic limit of the material ϵ_{nn}^{EL} is equal to f_t / E^e . (Figure 1) schematizes the one-dimensional smeared crack model as a system represented by a conventional spring CS of stiffness E^e , connected in serial with two devices in parallel: a frictional device FD that slips when $\epsilon_{nn} > \epsilon_{nn}^{EL}$ and a special spring NS of negative tangent stiffness $-E_c^{tan} = \partial F / \partial \epsilon_{nn}^c$. Consequently, the constitutive relationship in the crack direction exhibits three states of tensile behaviour: linear elastic, cohesive and non-cohesive, as shown (Figure 2) and the (Equation 1):

$$\sigma_{nn} = \begin{cases} E^e \epsilon_{nn} & \text{if } \epsilon_{nn} \leq \epsilon_{nn}^{EL} \\ F(\epsilon_{nn}^c) & \text{if } \epsilon_{nn}^{EL} < \epsilon_{nn} \leq \epsilon_{nn}^{CL} \\ 0 & \text{if } \epsilon_{nn} > \epsilon_{nn}^{CL} \end{cases} \quad (1)$$

where the cohesive limit strain is indicated as ϵ_{nn}^{CL} . Instead, a linear elastic behavior in compression is preserved.

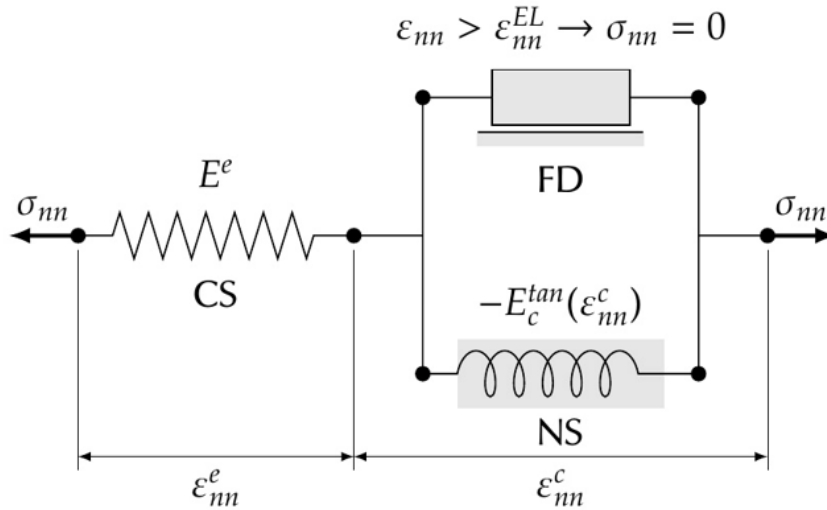


Figure 1. Schematic representation of a one-dimensional smeared crack model

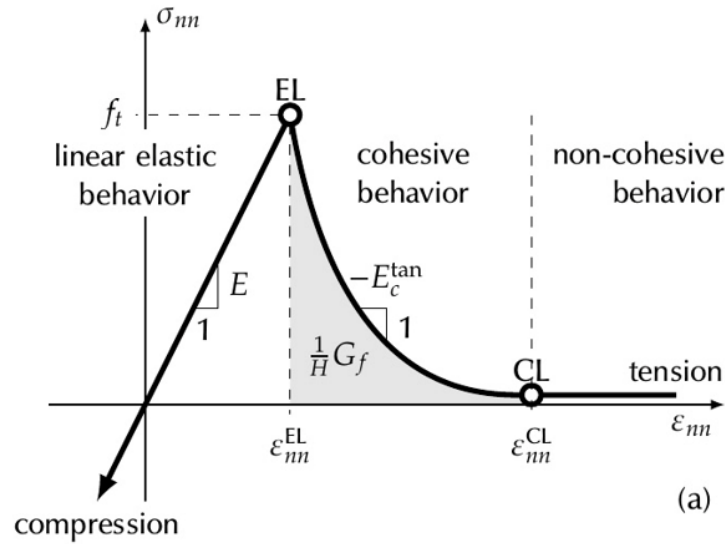


Figure 2. One-dimensional constitutive relationship in the crack direction

The cohesive behavior is defined by the experimental relationship between the crack opening W_m^c and the normal stress $\sigma_{nn} = L(W_m^c)$. This function is named softening law and is associated with the fracture energy per area unit in Mode-I. Some authors have obtained characteristic results of this function for plain concrete in accordance to bilinear (Petersson, 1981) or exponential functions (Hordijk, 1991); (Reinhardt et al., 1986). The cracking strain is related with the crack opening of the form $\varepsilon_{nn}^c = W_m^c / H$. The cracking process is distributed on the bandwidth H . In this numerical implementation, H depends on the projection of the finite element size over the major principal direction of the strain. Therefore, the one-dimensional relationship between the cracking strain and the normal stress is defined by the softening law and the parameter H .

2.2 Formulation of the constitutive model

The three-dimensional constitutive model for plain concrete establishes that the stress tensor σ depends on the strain tensor ε , the normal vector to the crack plane n , and the cracking strain ε_{nn}^c (Jirasek and Zimmermann, 2001) (Equation 2) thus:

$$\sigma = E^e : (\varepsilon - (n \otimes n) \varepsilon_{nn}^c) \tag{2}$$

where E^e is the elastic constitutive tensor. According to Rankine criteria, the normal crack orientation n is equal to the direction of the major principal strain $p^{(1)}$. The rotating crack model establishes that the crack orientation is tested in each loading step.

The normal stress on the plane with normal vector n can be expressed as $\sigma_{nn} = n \cdot \sigma \cdot n = (n \otimes n) : \sigma$, where the tensor σ is indicated in (Equation 2). Likewise, a softening law defines this component of stress. Consequently, (Equation 3)

$$(n \otimes n) : E^e : (\varepsilon - (n \otimes n) \varepsilon_{nn}^c) = L(H \varepsilon_{nn}^c) \tag{3}$$

The cracking strain ε_{nn}^c is computed from the analytical or numerical solution of the previous equation when softening law is bilinear or exponential, respectively (Tamasco, 2019).

The tangent constitutive relationship $\dot{\sigma} = E^{tan} : \dot{\varepsilon}$ relates the rate tensor of stress $\dot{\sigma}$ and strain $\dot{\varepsilon}$. The tangent constitutive tensor is equal to (Equation 4):

$$E^{tan} = E^e - (E^e : N) \varepsilon_{nn}^c - \left[\frac{E^e : n \otimes n \otimes n \otimes n : E^e}{\lambda + 2\nu + E_c^{tan}} \right] \tag{4}$$

where, \mathbf{N} is a fourth-order tensor associated to the directions $\mathbf{p}^{(1)}$, $\mathbf{p}^{(2)}$ and $\mathbf{p}^{(3)}$ of the principal strains ε_1 , ε_2 and ε_3 . This tensor corresponds to (Equation 5):

$$\begin{aligned}\mathbf{N} &= \left(\frac{2}{\varepsilon_1 - \varepsilon_2} \right) \mathbf{N}^{(12)} + \left(\frac{2}{\varepsilon_1 - \varepsilon_3} \right) \mathbf{N}^{(13)} \\ \mathbf{N}^{(12)} &= (\mathbf{p}^{(1)} \otimes \mathbf{p}^{(2)})^{\text{sym}} \otimes (\mathbf{p}^{(1)} \otimes \mathbf{p}^{(2)})^{\text{sym}} \\ \mathbf{N}^{(13)} &= (\mathbf{p}^{(1)} \otimes \mathbf{p}^{(3)})^{\text{sym}} \otimes (\mathbf{p}^{(1)} \otimes \mathbf{p}^{(3)})^{\text{sym}}\end{aligned}\quad (5)$$

The model is simplified to plane stress condition considering that the crack orientation \mathbf{n} , the principal stresses and the principal strains are contained in the plane. Consequently, the tensor \mathbf{N} reduces to (Equation 6):

$$\mathbf{N} = \left(\frac{2}{\varepsilon_1 - \varepsilon_2} \right) (\mathbf{p}^{(1)} \otimes \mathbf{p}^{(2)})^{\text{sym}} \otimes (\mathbf{p}^{(1)} \otimes \mathbf{p}^{(2)})^{\text{sym}} \quad (6)$$

2.3 Implementation of constitutive model in the FEM

A new constitutive material model is implemented into the open source nonlinear finite element analysis software HYPLAS (de Souza et al., 2008). Routines in Fortran language compute the stress and tangent constitutive tensor of the model and with these the internal force and stiffness matrices of the linear triangular finite element are obtained (Tamascio, 2019). The parameters of this model are: Young modulus \mathbf{E} , Poisson relation ν , the tensile strength f_t , and the fracture energy per area unit in Mode-I G_f . A softening law can be chosen among bi-linear, exponential or Reinhardt-Hordijk (RH). If the last is selected then two more coefficients are needed (Reinhardt et al., 1986).

3. Results of numerical simulation of concrete beams

The fracture process in three experimental tests of concrete beams subjected to bending was simulated with the implemented model. In the results, the clustering of the displacement contour lines inside a finite element band represents the cracking zone. Likewise, the relationship between a representative displacement and the applied load shows the structural response of the beam. Other result is the crack opening in each finite element. These experiments were previously tested and simulated by other authors.

3.1 Concrete beam of three points and one notch

A simply supported concrete beam is subjected to a point load P at the upper face of its half span, as shown in (Figure 3a). The representative displacement δ is the vertical component at the loading point. The beam has a notch of 100 mm of depth and 20 mm of thick. This test was carried out by (Petersson, 1981) to determinate the cracking process of the concrete in fracture Mode-I.

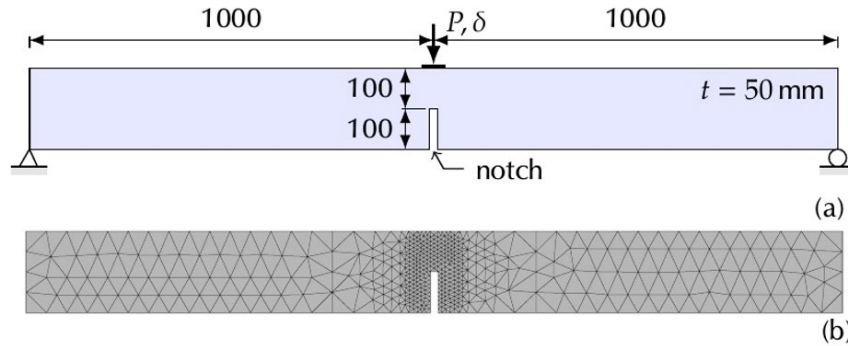


Figure 3. Concrete beam of three points and one notch: (a) geometry, support conditions and applied load (Petersson, 1981), and (b) finite element mesh. The units are given in mm

The domain of the test is represented by an unstructured mesh, which has 540 nodes and 946 linear triangular finite elements, as shown in (Figure 3b). The vertical displacement is applied in 1491 increments.

(Figure 4) shows the structural response of the concrete beam as the relationship between the load P and the displacement δ . This response is computed with the implemented numerical model using the three softening laws and compared with the envelope of the experimental tests presented (Petersson, 1981). The numerical results are close to the experimental tests; particularly, the curve of the simulation with the exponential softening law is inside the experimental result region.

The structural response of (Figure 4) and the crack opening W_{cnn} with deformed shape of (Figure 5) are presented in the representative steps A, B, C and D. Step A indicates the end of the linear behavior and the beginning of the fracture process at the notch tip, when the first finite element shows a crack opening greater than zero. The maximum load $P_{max}=710$ N is reached in step B, at the same time that the crack is propagated in a vertical direction up to 40% of the beam height. Step C represents the ending of the experimental tests, whereby the load decreases to $P=0.19P_{max}$ and the crack achieves the 90% of the beam height. In step D, the load is and the crack is extended throughout the beam height.

(Rots et al., 1985) simulated this experimental test with linear and bilinear softening, exhibiting similarity with the results of the implemented approach of the relationship between the load and the displacement at the midway of the beam.

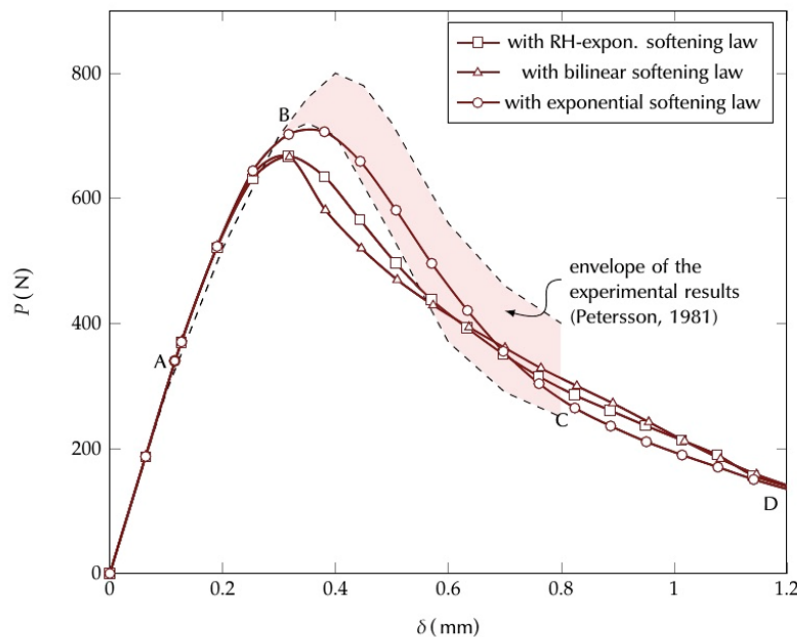


Figure 4. Concrete beam of three points and one notch: structural response computed in the numerical simulation and indicated by the experimental test (Petersson, 1981)

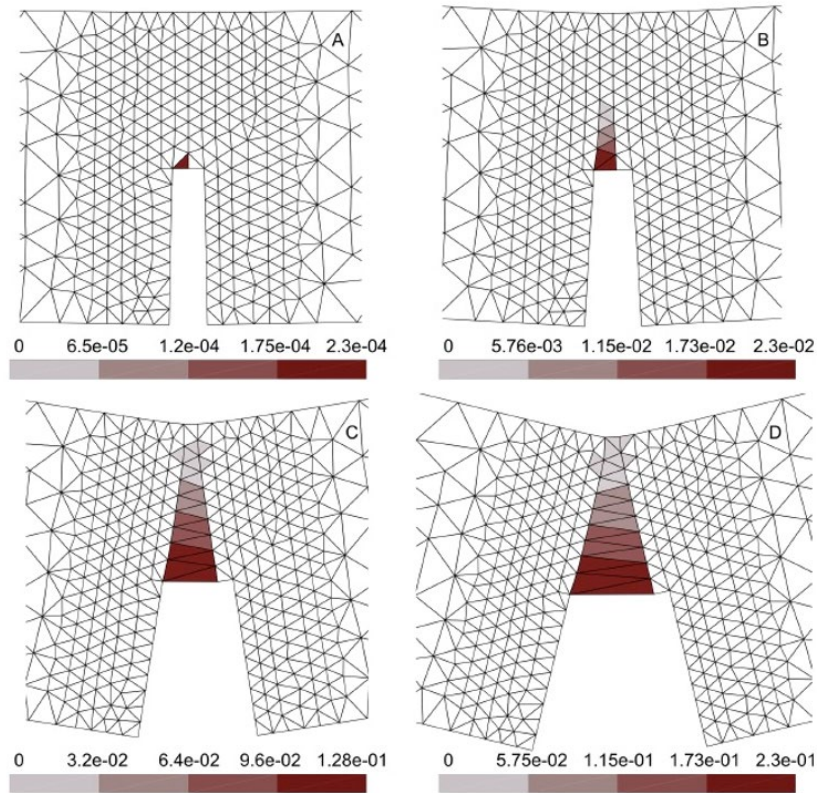


Figure 5. Concrete beam of three points and one notches: evolution of the deformed shape and the crack opening W_m in mm

3.2 Concrete beam of four points and one notch

A concrete beam with one notch is supported at two points and is subjected to the loads $0.13P$ and $1.0P$ transferred by a steel beam, as shown in (Figure 6). The relative vertical displacement between the bottom ends of the notch is measured in the test. This experimental test was established by (Arrea and Ingraffea, 1982), and then it was repeated by (Galvez et al., 2001). In this last work, the concrete mechanical properties correspond to: Young modulus $E = 24800$ MPa, Poisson relation $\nu = 0.18$, the tensile strength $f_t = 3.7$ MPa and the fracture energy per area unit $G_f = 0.13$ N/mm.

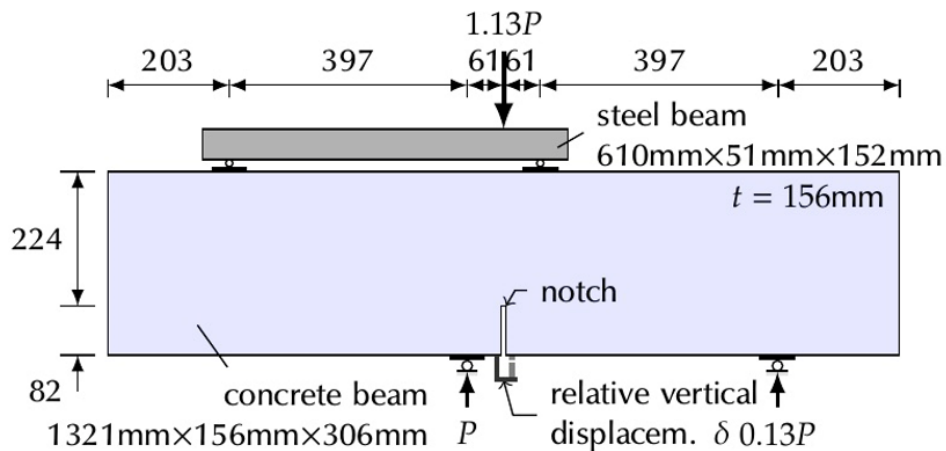


Figure 6. Beam of four points and one notch: geometry, support conditions and applied load. The units are given in mm. Adapted from (Galvez et al., 2001).

The concrete and steel beams are represented by an unstructured mesh with 1701 nodes and 3186 linear triangular finite elements, which is refined near three points: the right support of the steel beam, the left support of the concrete beam and the notch, as shown in (Figure 7). A vertical displacement was applied on the steel beam of incremental form in 1500 steps, achieving a relative vertical displacement at the notch greater than the experimental result.

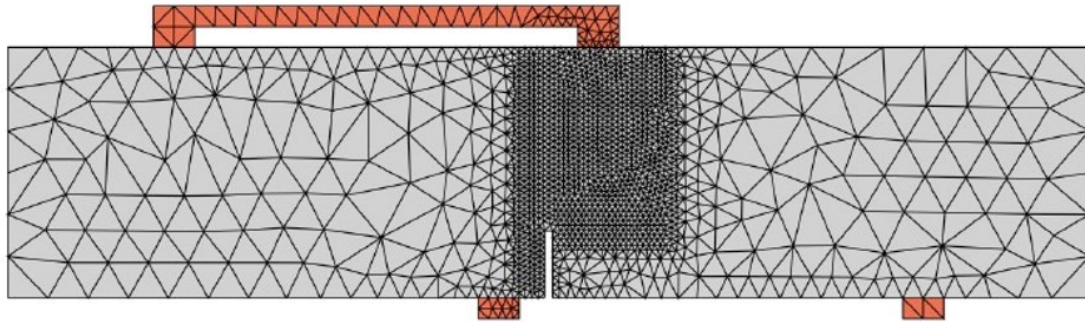


Figure 7. Beam of four points and two notches: finite elements mesh

The relationship between P and δ is computed, considering the Reinhardt-Hordijk (RH), exponential and bi-linear softening laws, as shown in (Figure 8). The structural responses obtained with RH-exponential and bi-linear softening laws are similar in comparison with the exponential law. These numerical responses are close to the lower limit of the experimental results (Galvez et al., 2001).

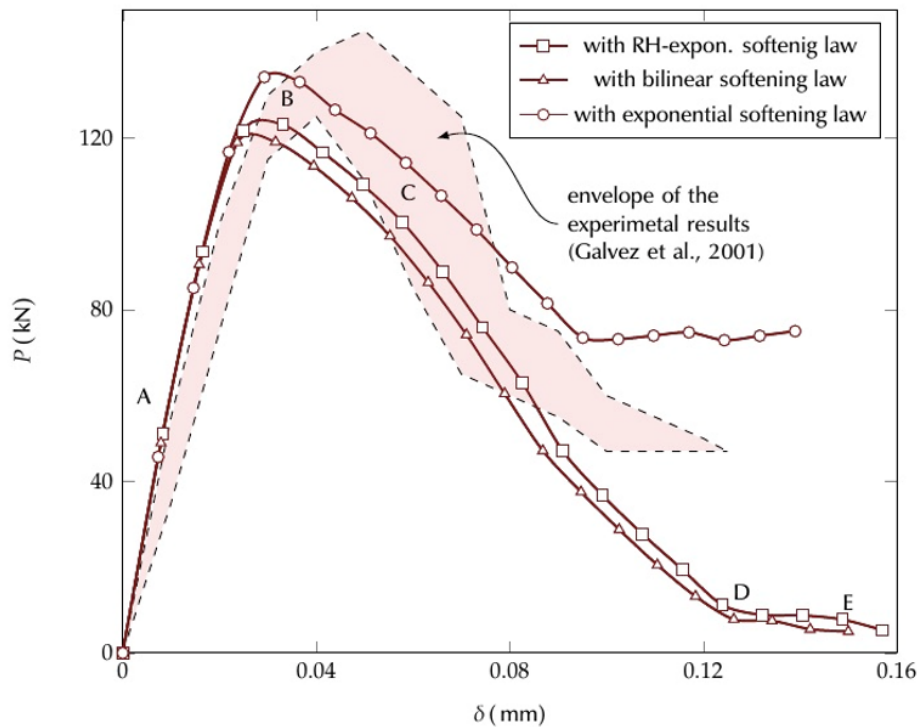


Figure 8. Beam of four points and one notch: structural response computed in numerical simulation and the experimental test

The steps A, B, C and D in (Figure 8) and (Figure 9) are representative instants of the structural response and the crack opening of the beam. The cracking begins at the notch tip, as shown in step A. Later in step B, the maximum load of the beam is reached above $P=125$ kN and the crack is propagated near the 30% of the height. The post-peak behavior shows a load decrease while the relative displacement, the crack opening, and the crack pattern increase. In step C, the load is reduced to 105 kN and the crack reaches the 85% the beam height. In step D the load is negligible and the crack crosses the entire beam height.

ENGLISH VERSION.....

The crack pattern is computed by the numerical simulation and is compared with the envelope of several experimental tests

(Cendon et al., 2000), (Galvez et al., 2001). (Figure 10) shows the similarity between these results, through a graph with origin at the bottom end of the notch.

(Rots et al., 1985) also simulated this experimental test, showing differences in the softening branch of the mechanical response with respect to the experimental test, due to no objectivity of the mesh orientation. Instead, the numerical model of (Cendon et al., 2000) reached a mechanical response and a crack pattern similar to the experimental results.

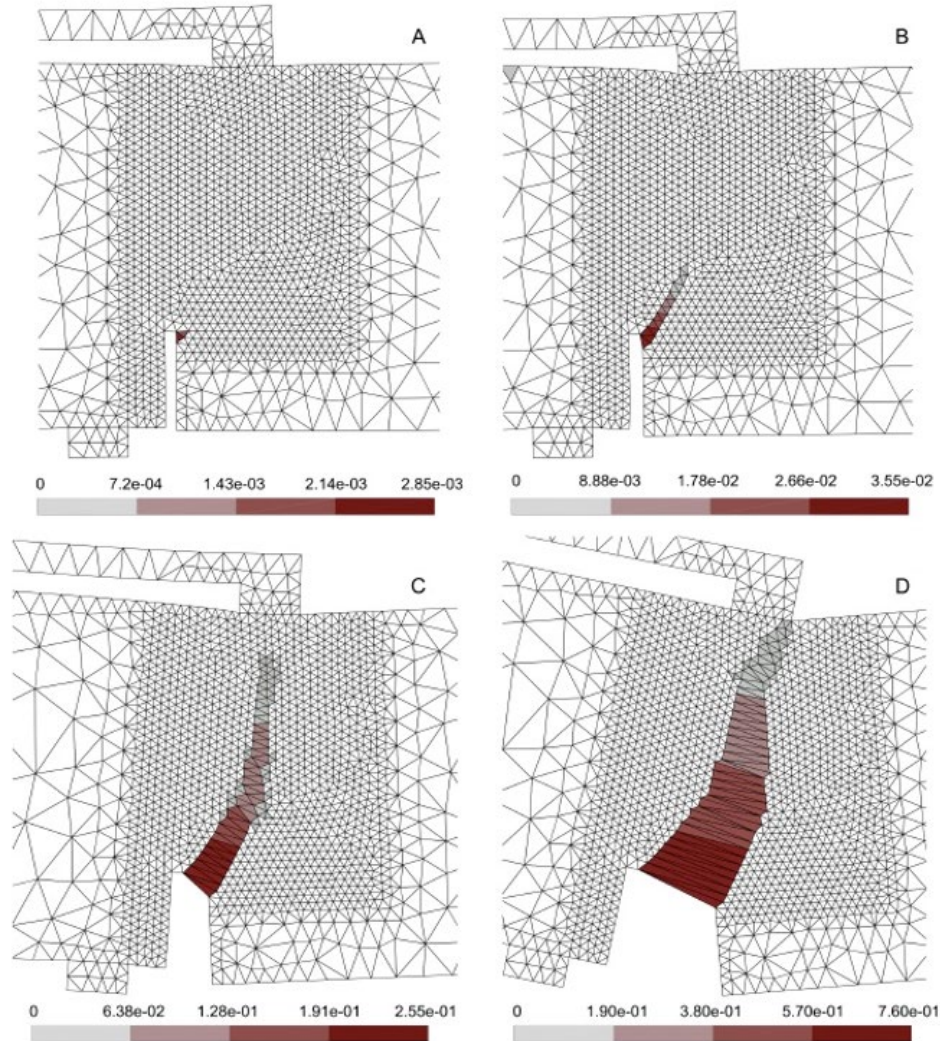


Figure 9. Beam of four points and one notch: evolution of the deformed shape and the crack opening

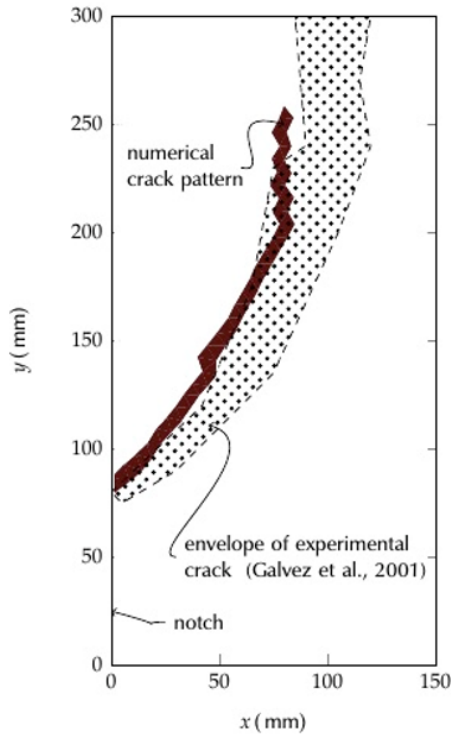


Figure 10. Beam of four points and one notch: crack pattern computed by the numerical simulation and obtained by the experimental tests

3.3 Concrete beam of four points and two notches

The implemented model is used to simulate the fracture process of a concrete beam with two notches, two point loads and two support points, as shown in (Figure 11). This benchmark was defined as the four points beam and tested by (Bocca et al., 1990).

The beam is 800 mm long, 200 mm height, 100 mm thick, and has two notches with 40 mm of depth. A load of $1.2P$ is applied on a steel beam, which transfers two loads of magnitudes $0.2P$ and $1.0P$ in the left and right contact points with the concrete beam, respectively. This configuration of the beam produces a mixed-mode fracture and two cracks, in which the bending and shear behavior are present simultaneously, in other words, fracture mode-I and -II.

The mechanical properties of the concrete were defined in the reference as Young modulus $E=27000\text{Mpa}$, tensile strength $f_t=2.0\text{MPa}$ and the fracture energy per area unit $G_f=0.10\text{N/mm}$. Instated, a Poisson relation $\nu=0.18$ is assumed.

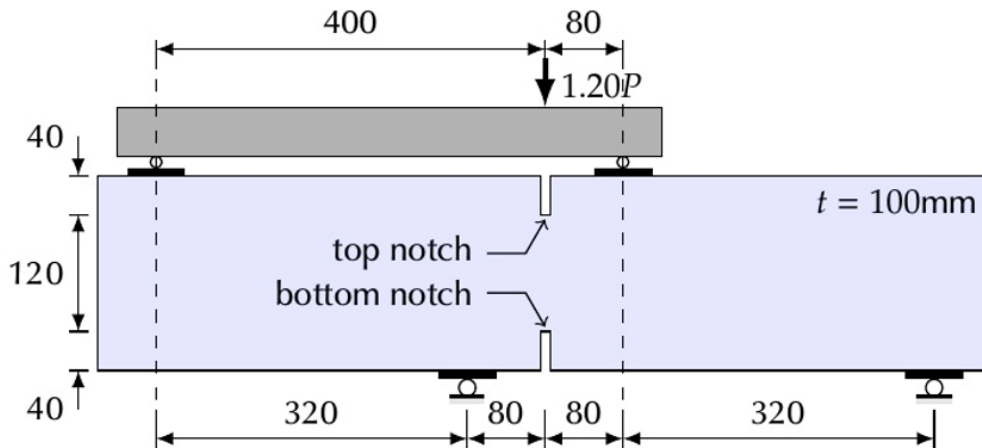


Figure 11. Beam of four points and two notches: geometry, support conditions and applied load. The units are given in mm. Adapted

ENGLISH VERSION.....

from Bocca and collaborators (Bocca et al., 1990)

Initially, the domain was represented by 3356 linear triangular finite elements, which are smaller near the notches. The mesh in this zone is shown in (Figure 12a). The bilinear and RH softening law represented the concrete behavior. The simulation with the RH softening law showed fewer amount of iterations per step and a small difference in the structural response, compared with the bilinear softening law. In consequence, the RH softening law is used in the next simulations.

Thereafter, three simulations were carried out with coarse, medium and fine mesh of linear triangular finite elements. These meshes had a non-structured distribution, avoiding the crack path tendency through the element sides. The number of elements and nodes, and the distribution of the meshes in the zone near the notches is presented in the first three columns of (Table 1) and in (Figure 12a), (Figure 12c), and (Figure 12e).

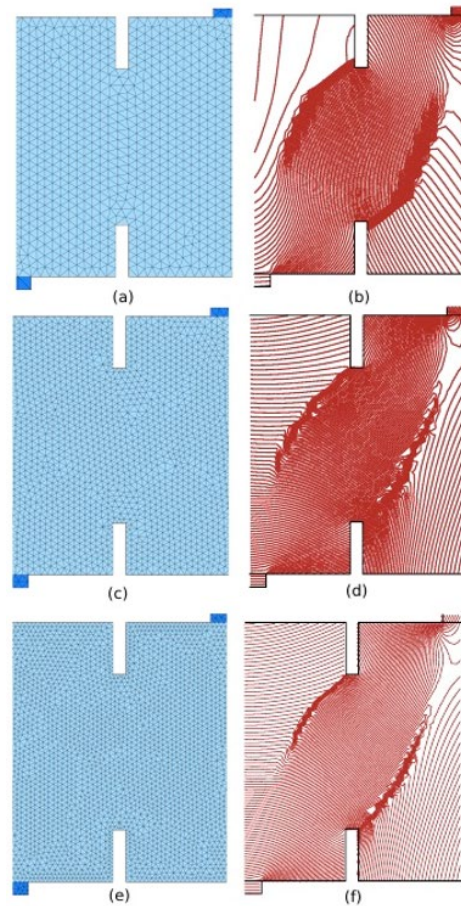


Figure 12. Beam of four points and two notches. Detail of central portion of the finite element mesh and displacement contour lines when the two cracks occur for: the coarse mesh in (a) and (b), the medium mesh in (c) and (d), and the fine mesh in (e) and (f), respectively

The experimental test shows a relationship between the load P applied in the right support of the steel beam (Figure 11) and a relative displacement δ . The location and the direction of the latter is not clear in the reference (Bocca et al., 1990). For this reason, we compared only the maximum load P_{max} from the experimental test (34.5 kN) with the results from numerical simulations. (Table 1) shows the maximum load P_{max} obtained for each mesh and the error rate with respect to experimental result. The difference is less than 10% in all cases, which is considered reasonable.

The clustering of displacement contour lines in the loading steps allows to represent the cracks. First, one crack begins at the tip of the top notch and grows downwards. Afterwards, other crack begins at the tip of the bottom notch and grows upwards. (Figure 12b), (Figure 12d), and (Figure 12f) show the displacement contour lines at the time that the two cracks are open for the coarse, medium and fine meshes, respectively.

Table 1. Beam of four points and two notches. Characteristics, maximum load P_{max} and error rate for three finite element meshes

ENGLISH VERSION.....

mesh	elements	nodes	steps	P_{max} (kN)	error (%)
coarse	3356	1798	87	31.59	8.4
medium	5189	2746	94	31.17	9.6
fine	8128	4253	64	32.19	6.7

The numerical result in all three meshes is similar and matches the experimental crack pattern obtained by Bocca and collaborators (Bocca et al., 1990), as shown in (Figure 13). These same authors also simulated the test with a remeshing technique of finite elements, obtaining a crack pattern alike.

Contrarily, fine meshes with a particular orientation of the element sides were simulated, showing incorrect crack patterns and errors of the maximum load greater than 20%. This lack of mesh objectivity (Bazant and Planas, 1998); (Jirasek and Zimmermann, 2001) has been overcome by the irregularity of the mesh. However, other strategies as crack tracking techniques preserve the mesh objectivity (Burnett and Schreyer, 2019); (Cervera and Chiumenti, 2006).

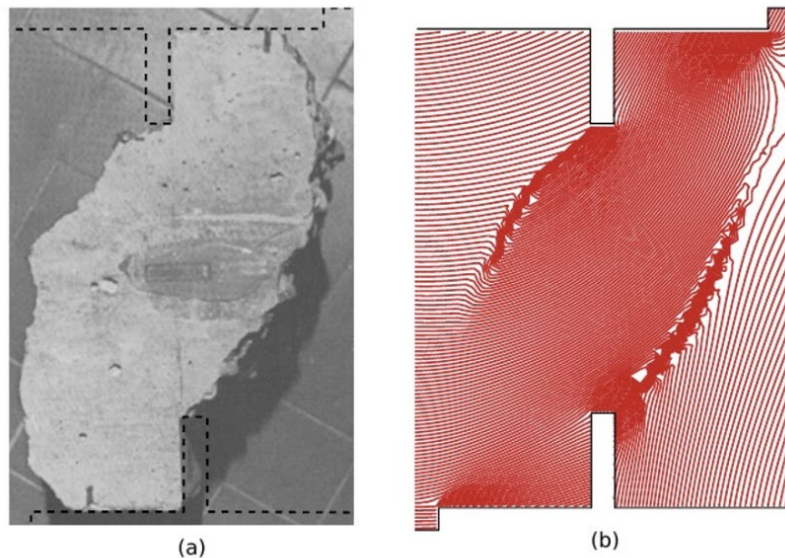


Figure 13. Beam of four points and two notches: (a) cracked block of beam from experimental test, and (b) displacement contour lines in the fine mesh when the two cracks occur

3.4 Final discussion

Three experimental tests of concrete beams with fracture mode-I and mixed mode were simulated through a finite element nonlinear analysis that includes a smeared crack model. In these simulations, the mechanical response and crack pattern were compared with the experimental results. (Table 2) indicates some characteristics of the numerical simulations of concrete beams simulated. In general, the similarity of the results was satisfactory. Furthermore, the maximum load difference between the numerical simulation and the experimental test was less than 10%.

Table 2. Summary of the three numerical simulations of concrete beams

Description	Fracture mode	Reference of the experimental test	Softening law with the closer to the experimental result	Similarity with the experimental test in: mechanical response / crack pattern / maximum load
Beam of three points and one notch	Mode-I	Petersson (1981)	Exponential	High / high / 90%
Beam of four points and one notch	Mixed-mode	Arrea and Ingraffea (1982), Galvez and others (2001)	RH-exponential	Medium / high / 94%
Beam of four points and two notches	Mixed-mode	Bocca, Carpinteri and Valente (1990)	RH-exponential	No applied / high / 92%

The crack opening was computed with this numerical model, showing the formation and the evolution of the fracture process. In the beams with three points and one notch and four points and one notch, after the maximum load (instant B), the opening crack and the

ENGLISH VERSION.....

cracked zone grows notoriously. Instead in instant C, the opening crack and the amount of finite elements over the notch of the beam are cracked. The simulation finishes at instant D, where whole the section over the notch of the beam is cracked and the opening crack is substantially increased. After instant D, a residual constant load is presented in the simulation, because the constitutive model does not have a damage threshold for tensile stress. Consequently, the compressive zone near the applied displacement does not fail and the normal stresses are redistributed near the crack sides.

The experimental tests were simulated with several unstructured meshes of different sizes and softening laws. Graphically, the displacement contours lines accumulated in a band of the size of one finite element, represent the crack pattern. This result is within the crack pattern zone of the experimental test.

Newton-Raphson scheme of nonlinear analysis showed numerical stability of the convergence of the solution. In the displacement steps of the simulations after the maximum load, about four iterations were required to reach the convergence. In other words, the displacement field, which complies with the equilibrium condition, is obtained with few iterations, despite the high value of the strain at the cracking zone during the softening behavior.

4. Conclusions

The rotating smeared crack model implemented in the nonlinear finite element analysis allows us to represent the fracture process of plain concrete in structures considering plane stress condition, static loads and infinitesimal strains. Particularly, the beams subjected to bending and shear exhibit similar results to the experimental tests performed by other authors. Results of the three tests showed satisfactory crack patterns and structural responses.

The product of this work is a computational code written in Fortran language and implemented on the open source software of two-dimensional nonlinear finite element analysis HYPPLAS. A new constitutive model based on the smeared crack formulation with three softening laws was included. The reading of the input data generated from the graphical pre-process module of the software GMSH and the writing of results for the graphical post-process module of the same program, were also implemented. GMSH, the used Fortran compiler and the code of this work are free software and compatible with Windows, Linux and Mac operating systems.

This work aids to understand the numerical formulation and implementation of the fracture process in concrete structural elements by means of finite element method and the smeared crack model.

The mechanical response and the crack pattern of structural members of reinforced concrete determine the design of buildings, bridges, walls and others subjected to extreme loading conditions. These structures kind could be simulated considering separately finite elements of plain concrete using the implemented model and of steel defined with a elasto-plastic model. Other way is considering finite elements of material composed of a volumetric percent of plain concrete and steel, represented by the implemented model and the mixing theory.

5. Recommends for research future

In the future, a constitutive model of composite material of concrete reinforced with bars or steel fibers could be formulated and implemented. This will allow the simulation of structural members of this material in a simplified two-dimensional form, depending on the steel percent. On the other hand, models that describe the Fracture Mode-II could be implemented, in order to represent the mechanical behavior of structures subjected mainly to shear stress.

6. References

- Arrea, M.; Ingraffea, A. R. (1982).** Mixed mode crack propagation in mortan and concrete.
- Bazant, Z.; Planas, J. (1998).** Fracture and size effect in concrete and other quasibrittle materials. CRC Press.
- Bocca, P.; Carpinteri, A.; Valente, S. (1990).** Size effects in the mixed mode crack propagation: Softening and snap-back analysis. *Engineering Fracture Mechanics*, 35(1-3), 159-170.
- Burnett, D. J.; Schreyer, H. L. (2019).** A mesh objective method for modeling crack propagation using the smeared crack approach. *International Journal for Numerical Methods in Engineering*, 117(5), 574-603.
- Cervenka, V. (1985).** Constitutive model for cracked reinforced concrete. *ACI Journal*, 82, 877-882.
- Cervera, M.; Chiumenti, M. (2006).** Mesh objective tensile cracking via a local continuum damage model and a crack tracking technique. *Computer Methods in Applied Mechanics and Engineering*, 196, 304-320. <https://doi.org/10.1016/j.cma.2006.04.008>
- Cendon, D. A.; Elices, M.; Garlvez, J.C. (2000).** Modelling the fracture of concrete under mixed loading. *International Journal of Fracture*, 103, 293 - 310.
- CIMNE. (2000).** GiD Reference manual. Barcelona: International Center For Numerical Methods In Engineerin (CIMNE).
- de Borst, R.; Nauta, P. (1985).** Non-orthogonal cracks in smeared finite element model. *Engineering Computation*, 2(1), 35-46. <https://doi.org/doi.org/10.1108/eb023599>
- de Borst, R.; Remmers, J. J. C.; Needleman, A.; Abellan, M.-A. M.-A. (2004).** Discrete vs smeared crack models for concrete fracture: bridging the gap. *International Journal for Numerical and Analytical Methods in Geomechanics*, 28(7-8), 583-607.

ENGLISH VERSION.....

<https://doi.org/10.1002/nag.374>

- de Souza, E. A.; Peric, D.; Owen, D. R. (2008).** *Computational methods for plasticity*. Wiley.
- Galvez, J. C.; Cendon, D.; Elices, M. (2001).** *Mixed mode fracture of double-edge notched specimens of concrete*. In R. de Borst, P.-C. G. Mazars J., J. van Mier (Eds.), *Fracture Mechanics of Concrete Structures IV* (pp. 349–356). Rotterdam, The Netherlands: Balkema Publishers.
- Geuzaine, C.; Remacle, J. F. (2009).** *Gmsh: a three-dimensional finite element mesh generator with built-in pre- and post-processing facilities*. *International Journal for Numerical Methods in Engineering*, 79(11), 1309–1331.
- Graffe, R.; Linero, D. (2010).** *Numerical modeling of the fracture process in mode I of concrete beams with known cracking path by means of a discrete model of cohesive crack*. *Revista de Ingeniería de Construcción*, 25(3), 399–418.
- Hordijk, D. A. (1991).** *Local approach to fatigue of concrete*. Delf University of Technology.
- Jirasek, M.; Patzak, B. (2001).** *Models for quasibrittle failure: theoretical and computational aspects*. In *European Conference on Computational Mechanics*.
- Jirasek, M.; Bauer, M. (2012).** *Numerical aspects of the crack band approach*. *Computers & Structures*, 110–111, 60–78. <https://doi.org/https://doi.org/10.1016/j.compstruc.2012.06.006>
- Jirasek, M.; Zimmermann, T. (2001).** *Embedded crack model. Part II: combination with smeared cracks*. *International Journal for Numerical Methods in Engineering*, 50(6), 1291–1305.
- Oliver, J. (1989).** *A consistent characteristic length for smeared cracking models*. *International Journal for Numerical Methods in Engineering*, 28, 461–474.
- Oliver, J. (1996).** *Modelling Strong Discontinuities in Solid Mechanics Via Strain Softening Constitutive Equations. Part 2: Numerical Simulation*. *International Journal for Numerical Methods in Engineering*, 39(21), 3601–3623. [https://doi.org/10.1002/\(SICI\)1097-0207\(19961115\)39:21<3601::AID-NME64>3.0.CO;2-4](https://doi.org/10.1002/(SICI)1097-0207(19961115)39:21<3601::AID-NME64>3.0.CO;2-4)
- Petersson, P. E. (1981).** *Crack growth and development of fracture zones in plain concrete and similar materials*. Lund University, Division of Building Materials, Lund Institute of Technology.
- Rashid, Y. (1968).** *Analysis of prestressed concrete pressure vessels*. *Nuclear Engineering and Design*, 7, 773–782.
- Reinhardt, H. W.; Hordijk, D. A.; Cornerlissen, H. A. W. (1986).** *Experimental Determination of Crack Softening Characteristics of Normalweight and Lightweight*. *Heron*, 31(2), 45–56.
- Rots, J. G.; Blaauwendraad, J. (1989).** *Crack models for concrete: discrete or smeared? fixed, multi-directional or rotating?* *Heron*, 34(1), 1–59.
- Rots, J. G.; Nauta, G. M.; Kuster, M. A.; Blaauwendraad, J. (1985).** *Smeared crack approach and fracture localization in concrete*, *Heron*, 30(1), 1–48.
- Sakbana, A.; Mashreib, M. (2020).** *Finite Element Analysis of CFRP- Reinforced Concrete Beams*, *Revista de Ingeniería de Construcción*, 35(2), 148-169.
- Suidan, M.; Schnobrich, W. C. (1973).** *Finite element analysis of reinforced concrete*. *American Society of Civil Engineers*, 99(10), 2109–2122.
- Tamasco, J. C. (2019).** *Simulación del proceso de fractura de estructuras de concreto simple, con el modelo de fisura distribuida rotante en el marco del método de los elementos finitos*. Universidad Nacional de Colombia.
- Vecchio, F.; Collins, M. (1986).** *The modified compression-field theory for reinforced concrete elements subjected to shear*. *ACI Journal*, 83(2), 219–231.
- Zi, G.; Belytschko, T. (2003).** *New crack-tip elements for XFEM and applications to cohesive cracks*. *International Journal for Numerical Methods in Engineering*, 57(15), 2221–2240. <https://doi.org/10.1002/nme.849>
- Zienkiewicz, O. C.; Taylor, R. L.; Zhu, J. Z. (2013).** *The Finite Element Method (7th ed., Vol. Volume 1)*. Oxford: Elsevier.